J. CHEM. SOC. FARADAY TRANS., 1991, 87(17), 2855–2859

Distribution of Cations in Lanthanum-exchanged NaY Zeolites

Der-Shiuh Shy, Shiann-Horng Chen, Jan Lievens,† Shang-Bin Liu‡ and Kuei-Jung Chao*
Department of Chemistry, National Tsinghua University, Hsinchu, Taiwan, Republic of China

The locations of the exchangeable cations of partially La-exchanged NaY zeolites (Si/Al = 2.29) in dehydrated and rehydrated states have been determined using powder X-ray diffraction and ^{129}Xe NMR and from the isotherm of adsorbed xenon.

Most the La^{3+} ions in LaNaY tend to migrate irreversibly from supercages into sodalite cages or hexagonal prisms, while the Na^+ ions prefer to stay in the supercages after sample dehydration treatment at 350 °C. Sites I and II are occupied by La^{3+} and Na^+ ions, respectively, while both Na^+ and La^{3+} ions are located at site I′. The amount of La^{3+} ions in sodalite cages increases with the increase of La content and the readsorption of water. The occupancy of Na^+ ions at site II was found to decrease with increasing degree of La exchange from both X-ray diffraction studies and from the xenon adsorption isotherm. ^{129}Xe NMR results indicate that the nature of intersupercage void space is similar for LaNaY and NaY.

The rare-earth forms of Y zeolites (REY) exhibit high thermal stability, acidity and have been extensively employed in petroleum-refining processes.[1,2] The Brønsted acidity of REY, generated by the hydrolysis of the rare-earth cations at site I′ in sodalite cages, has been confirmed by adsorption of pyridine or amine,[3] IR[4] and neutron diffraction studies.[5] The interactions between the rare-earth cations located in small sodalite cages or hexagonal prism (site I) cages and the anionic zeolite framework play important roles in stabilizing the framework structure when the sample is subjected to heat treatment.[6] Despite extensive structure studies on La-exchanged Y zeolites under different heat treatment,[5–10] very little attention has been devoted to studying the effects of the degree of cation exchange on the cation distribution.[8,11–13] For LaNaY zeolite samples obtained by low-temperature (≤60 °C) La^{3+}–NaY ion exchange,[14] the hydrated La^{3+} ions are restricted to supercages. During heating and dehydration, the La^{3+} ions (ionic diameter 0.23 nm) strip off their hydration shell and migrate from supercages into the small sodalite or hexagonal prism cavities.[11,15,16] The cation distribution in LaNaY zeolite should therefore vary with heat treatment and with lanthanum content. In this study, powder X-ray diffraction was employed to determine the correlation between cation distribution and lanthanum content on a series of dehydrated and rehydrated LaNaY zeolites.

For dehydrated LaNaY, the nature of the supercages was further investigated by xenon adsorption. Since xenon atoms with a diameter of 4.4 Å can be adsorbed only in the supercage and cannot enter the hexagonal prism, xenon adsorption has been shown to be a sensitive method for studying the geometric and electronic environment inside the supercage of Y zeolites.[17–19] The distortion of the xenon electron cloud arising from its collision with the framework wall, cations or other xenon atoms in supercages is displayed in the ^{129}Xe (spin 1/2) NMR chemical shift[17] and linewidth, while the effect of cations on xenon adsorption may be reflected in the adsorption isotherm.

Experimental

Sample Preparation

The binder-free polycrystalline zeolite NaY (Si/Al = 2.29) was obtained from Strem Chemical Co. To avoid a possible deficiency in cations, the powdery sample was sequentially washed with 1 mol dm^{-3} NaCl solution and deionized water, then dried at room temperature before ion exchange. Ion exchange was carried out by mixing the NaY zeolite with lanthanum chloride solution at room temperature. In order to remove residual salt, the samples were washed with deionized water until they were free of Cl^- ions as detected by $AgNO_3$ solution. All zeolite samples were then air-dried and stored over saturated NH_4Cl solution at room temperature. The samples were digested with mixed acid and their chemical compositions were determined by inductively coupled plasma atomic emission spectrometry (ICP-AES).[20] The percentage of La^{3+} exchanged in the zeolites is denoted as prefix for the samples, *e.g.* 68LaNaY indicates 68% of Na being replaced by La.

Collection of X-Ray Diffraction Data

LaNaY powder without binder was pressed into a pellet of 12 × 15 mm and mounted in a HDK (Seifert) high-temperature X-ray diffractometer camera. After dehydration at room temperature and under vacuum (diffusion pump), the temperature was raised to 350 °C over 12 h and held at 350 °C for another 12 h at a final pressure of 10^{-6} Torr.† The diffraction pattern was recorded at 350 °C in two parts, using an automatic powder diffractometer (Seifert–Scintag Pad II) with Ni-filtered Cu-Kα radiation in steps of 0.01°, 2Θ (opening angle 1–2° of the incident beam and 4 s counting times between 4°–40°, 2Θ and 3–4° and 8 s counting time between 30–80°). The spectra were scaled to each other using the overlapping part for 2Θ = 33–39°. The rehydrated sample was obtained by exposing the dehydrated sample to air and its diffraction pattern was recorded in the same way as for the dehydrated ones.

The X-ray data-sampling and refinement procedures have been described extensively elsewhere.[21,22] In brief, the agreement factors (R_G and wR_G) can be defined as:

$$R_G = \frac{\sum ||G^o| - |G^c||}{\sum |G^o|}$$

$$wR_G = \left(\frac{\sum (w^{1/2} ||G^o| - |G^c||)^2}{\sum (w^{1/2} |G^o|)^2} \right)^{1/2}$$

where $w = 1/\sigma^2_{G^o}$ and G is F_{hkl} or I_N, *i.e.* the sum of intensities for all coinciding reflections ($N = h^2 + k^2 + l^2$), the superscript o denotes observed and c calculated values and σ is the standard deviation.

† Present address: Centrum voor Oppervlaktecheikunde en Katalyse, K.U. Leuven, Kard. Mercierlaan 92, B-3001 Heverlee, Belgium.

‡ Present address: Institute of Atomic and Molecular Sciences, Academia Sinica, P.O. Box 23-166, Taipei 10764, Taiwan, R.O.C.

† 1 Torr = 101 325/760 Pa.

Xenon Adsorption Isotherm Measurements

A known amount of zeolite (typically *ca.* 1 g) was loaded into a 10 mm NMR tube with an attached vacuum valve. Before isotherm measurement, the sample was evacuated to *ca.* 2×10^{-4} Torr for 3 days at room temperature, it was then heated to 350 °C with a heating rate of 0.2 °C min^{-1}, and maintained at this temperature for $\geqslant 30$ h (2×10^{-5} Torr). All the xenon adsorption isotherms were measured by the volumetric method at 22 °C.

^{129}Xe NMR Measurements

^{129}Xe NMR spectra of adsorbed xenon were obtained on a Bruker MSL-300 spectrometer operating at 83.0 MHz and 295 K. Typically 2000–40000 signal acquisitions were accumulated for each spectrum with a recycle delay of 0.3 s between each radiofrequency pulse. The ^{129}Xe NMR chemical shifts were referenced to that of external xenon gas extrapolated to zero pressure using Jameson's equation.[23] All resonance signals of xenon adsorbed in zeolites were shifted downfield from the reference which is defined as the positive direction in this report.

Results and Discussion

X-Ray Diffraction

Positional parameters, population factors, isotropic temperature factors, agreement factors and unit-cell parameters of dehydrated 21LaNaY, 41LaNaY, 68LaNaY and rehydrated 68LaNaY are compiled in Table 1. A summary of the site populations, and a list of selected intra-atomic distances and bond angles are given in Tables 2 and 3, respectively. The unit-cell sizes of the dehydrated LaNaY are higher than those for dehydrated NaY[24] but show no obvious relationship with the level of La exchange. A list of observed and calculated structure factors is available on request.

There are 16 sites I per unit cell in Y zeolites, the sites I′, II and II′ have the same multiplicity of 32 per unit cell. Dendooven *et al.*[25] found that the occupancy of the better co-ordinated sites is favoured at elevated temperatures, and the better co-ordinated cation site is site I in the dehydrated CaY zeolite. Based on a series of model calculations, Van Dun *et al.*[26] concluded that the site preferences are I > II > I′ for monovalent cations and I > I′ > II for divalent cations in dehydrated Y zeolites. Since site I is energetically the most favourable for monovalent and divalent cations,[25–27] it might be the most favourable site for trivalent cations also.

Since the association energy of the lanthanum ion and the faujasite framework (−3000 kJ mol^{-1}) is greater than that for the sodium cation (−393 kJ mol^{-1}) in the dehydrated state,[28,29] the lanthanum ion is more preferred than the sodium ion in LaNaY zeolites for occupancy of site I. On the other hand, the number of orbital electrons in lanthanum is *ca.* 6.5 times greater than that of sodium[6] and this should be considered on assigning the occupancy of cation sites. The observed count of electrons for site I is greater than the estimated values for all the sodium atoms in d-41LaNaY, d-

Table 1 Positional parameters,[a] population parameters (*p*), temperature factors ($B/10^{-2}$ nm^2), agreement factors and unit-cell parameters (Å) for d-NaY,[28] d-21LaNaY, d-41LaNaY, d-68LaNaY and r-68LaNaY (dehydrated at 350 °C)

		dNaY[b]	d-21LaNaY	d-41LaNaY	d-68LaNaY	r-68LaNaY
T = Si, Al	*X*	0.1246 (3)	0.1247 (2)	0.1245 (2)	0.1254 (2)	0.1256 (2)
(192i)[d]	*Y*	0.9453 (3)	0.9450 (2)	0.9445 (2)	0.9447 (2)	0.9451 (2)
	Z	0.0360 (3)	0.0363 (2)	0.0358 (2)	0.0352 (2)	0.0355 (2)
	B	1.9 (0.1)	1.3 (0.2)	1.8 (0.2)	1.9 (0.2)	1.4 (0.2)
O(1)	*X* = −*Y*	0.1064 (5)	0.1077 (4)	0.1090 (4)	0.1080 (4)	0.1074 (5)
(96h)	*Z*	0.0	0.0	0.0	0.0	0.0
	B	2.1 (0.7)	2.6 (0.4)	2.2 (0.4)	2.7 (0.4)	3.6 (0.5)
O(2)	*X* = *Y*	0.2527 (5)	0.2526 (4)	0.2534 (4)	0.2524 (4)	0.2515 (4)
(96g)	*Z*	0.1394 (7)	0.1392 (6)	0.1389 (6)	0.1389 (6)	0.1419 (6)
	B	2.6 (0.6)	1.4 (0.4)	1.3 (0.4)	3.5 (0.4)	1.6 (0.4)
O(3)	*X* = *Y*	0.1770 (5)	0.1776 (4)	0.1784 (4)	0.1768 (4)	0.1739 (4)
(96g)	*Z*	0.9648 (9)	0.9647 (6)	0.9630 (8)	0.9645 (6)	0.9640 (6)
	B	3.5 (0.6)	2.1 (0.4)	4.3 (0.5)	2.9 (0.4)	1.0 (0.4)
O(4)	*X* = *Y*	0.1776 (6)	0.1776 (5)	0.1771 (5)	0.1782 (4)	0.1807 (4)
(96g)	*Z*	0.3182 (9)	0.3193 (6)	0.3154 (7)	0.3169 (6)	0.3163 (6)
	B	4.9 (0.7)	2.5 (0.4)	3.0 (0.5)	2.5 (0.4)	1.5 (0.4)
O(II′)	*X* = *Y* = *Z*	—	0.1593 (30)	0.1666 (28)	0.1617 (25)	0.1637 (20)
(32e)	*P*	—	0.22 (0.10)	0.22 (0.10)	0.22 (0.07)	0.33 (0.10)
	B	—	3.0[c]	3.0[c]	3.0[c]	3.0[c]
La(I′)	*X* = *Y* = *Z*	—	—	0.0695 (3)	0.0662 (3)	0.0665 (2)
(32e)	*P*	—	—	0.06 (0.02)	0.24 (0.01)	0.33 (0.01)
	B	—	—	2.5 (3.5)	2.2 (0.5)	2.4 (0.4)
Na(I′)	*X* = *Y* = *Z*	0.0500 (12)	0.0609 (9)	0.0530 (6)	—	—
(32e)	*P*	0.42 (0.05)	0.63 (0.07)	0.22 (0.16)	—	—
	B	3.8 (2.3)	5.4 (1.6)	4.0 (5.2)	—	—
Na(II)	*X* = *Y* = *Z*	0.2341 (6)	0.2315 (5)	0.2333 (6)	0.2339 (6)	0.2368 (8)
(32e)	*P*	0.92 (0.05)	0.84 (0.06)	0.81 (0.05)	0.55 (0.04)	0.50 (0.05)
	B	3.5 (1.0)	4.1 (1.0)	5.4 (1.0)	1.4 (1.1)	2.5 (1.5)
La(I)	*X* = *Y* = *Z*	0.0	0.0	0.0	0.0	0.0
(16c)	*P*	0.48 (0.06)	0.24 (0.02)	0.37 (0.02)	0.28 (0.01)	0.16 (0.02)
	B	3.1 (2.6)	4.8 (1.1)	3.9 (0.6)	3.6 (0.7)	1.8 (1.2)
RI[e]		9.7	15.0	11.6	11.2	18.9
wRI		9.6	19.4	15.9	15.9	21.4
RF		9.0	6.9	7.1	6.2	12.7
wRF		5.0	13.6	11.6	10.6	17.2
a_0/Å[f]		24.800 (3)	24.829 (1)	24.807 (2)	24.814 (1)	24.816 (1)

[a] Space group *Fd3m*; standard deviation of the last digit is given in parentheses. [b] Dehydration at 450 °C, ref. 24. [c] Fixed during the refinement. [d] Multiplicity and Wyckoff letter. [e] Agreement factors. [f] Unit-cell parameter. d = dehydrated; r = rehydrated.

Table 2 Occupancy (no. of atoms per unit cell) of the sites I, I′, II′ and II for d-21LaNaY, d-41LaNaY, d-68LaNaY and r-68LaNaY

	d-21LaNaY	d-41LaNaY	d-68LaNaY	r-68LaNaY
site I (La)	3.8 (0.3)	5.9 (0.3)	4.5 (0.2)	2.6 (0.3)
site I′ (Na)	20.2 (2.2)	7.0 (5.1)	—	—
site I′ (La)	—	1.9 (0.6)	7.7 (0.3)	10.6 (0.3)
site II (Na)	26.9 (1.9)	25.9 (1.6)	17.6 (1.3)	16.0 (1.6)
site II′ (O)	7.0 (3.2)	7.0 (3.2)	7.0 (2.2)	10.6 (3.2)
Na (I′ + II)	47.1 (4.1)	33.9 (6.7)	17.6 (1.3)	16.0 (1.6)
La (I + I′)	3.8 (0.3)	7.8 (0.9)	12.2 (0.5)	13.2 (0.6)
Na + 3 La	58.5	57.3	54.2	55.6
calc. La exchange ratio (%)	20	41	68	71

Standard deviations of the last significant digit are given in parentheses.

68LaNaY and r-68LaNaY. The total amount of Na^+ ions at sites I and II then exceeds the estimated value for d-21LaNaY, if site I were assumed to be completely occupied by Na^+ ions. We therefore suggest that only lanthanum ions can be localized at site I. For highly La-exchanged NaY zeolites (dehydration at 350 °C), no cation was found to be located at site I,[6–8] except for samples dehydrated at temperatures $\geqslant$475 °C.[6,7,10]

Since both lanthanum and sodium cations can be present at site I′, the assignment of electron density could be ambiguous. However, considering the elemental composition, site I′ is likely to be occupied by sodium ions for d-21LaNaY, by lanthanum ions for d-68LaNaY and r-68LaNaY, and by both lanthanum and sodium ions for d-41LaNaY. As for the La—O (2.6 Å) and Na—O (2.4 Å) distances, the electron density at site I′ was deconvoluted into two parts (sodium and lanthanum) for d-41LaNaY, but not for d-21LaNaY and 68LaNaY. By comparing the cation distributions of d-68LaNaY with those of r-68LaNaY, the migration of lanthanum ion from site I to site I′ was observed upon adsorption of water. Although site I is energetically most stable in the dehydrated state, cations cannot occupy site I completely, owing to the repulsions between the cations at sites I and I′. The numbers of ions at site I are 3.8, 5.9 and 4.5, while the numbers of ions at site I′ are 20.2, 8.9 and 7.7 for d-21LaNaY, d-41LaNaY and d-68LaNaY, respectively. Relative to d-NaY (29.4 Na^+ at site II), the occupancies of Na^+ ions at site II are reduced by lanthanum substitution.

After dehydration, all lanthanum ions migrate from the supercages into the sodalite cages and hexagonal prisms, while sodium ions are localized at sites I′ and II. On adding up the lanthanum and sodium ions at sites I, I′ and II in Table 2, lanthanum-exchange ratios, which are consistent with the elemental compositions, may be obtained. The total numbers of La and Na ions from XRD analysis are in excellent agreement with the estimated values for 58.3 Al atom per unit cell, except for 68LaNaY, in which a little dealumination was found after dehydration, from ^{27}Al NMR.[30]

The framework tetrahedra are fairly regular (Table 3) and can be derived from the tetrahedral bond distances and bond angles. The average T—O distances are in close agreement with the weighted mean bond length of 1.65 Å calculated from Si/Al = 2.29, Si—O = 1.61 Å and Al—O = 1.74 Å. The T—O tetrahedra are indeed rather rigid, with O—T—O bond angles of *ca.* 109.45°.

According to Scherzer's results,[8] the influence of the cations upon the (Si, Al)—O bond lengths can be detected by the increase of the bond length. Comparing the bond length

Table 3 Selected interatomic distances (Å) and bond angles (°) for d-21LaNaY, d-41LaNaY, d-68LaNaY and r-68LaNaY

	d-21LaNaY	d-41LaNaY	d-68LaNaY	r-68LaNaY
T—O(1)	1.644 (7)	1.643 (8)	1.630 (7)	1.636 (8)
T—O(2)	1.660 (15)	1.656 (15)	1.645 (16)	1.661 (16)
T—O(3)	1.652 (17)	1.649 (20)	1.675 (18)	1.656 (16)
T—O(4)	1.629 (19)	1.614 (20)	1.621 (18)	1.630 (19)
mean	1.646	1.641	1.643	1.646
T—O(1)—T	135 (1)	132 (1)	135 (1)	137 (1)
T—O(2)—T	150 (1)	151 (1)	150 (1)	145 (1)
T—O(3)—T	140 (1)	141 (1)	142 (1)	145 (1)
T—O(4)—T	147 (1)	154 (1)	151 (1)	147 (1)
O(1)—T—O(2)	111 (1)	111 (1)	113 (1)	114 (1)
O(1)—T—O(3)	109 (1)	109 (1)	110 (1)	110 (1)
O(1)—T—O(4)	110 (1)	112 (1)	112 (1)	112 (1)
O(2)—T—O(3)	105 (1)	106 (1)	104 (1)	107 (1)
O(2)—T—O(4)	108 (1)	106 (1)	107 (1)	103 (1)
O(3)—T—O(4)	113 (0)	112 (0)	111 (0)	111 (0)
La(I)—6 O(3)	2.687 (16)	2.675 (14)	2.716 (16)	—
La(I)—2 Na(I′)	2.62 (3)	2.277	—	—
La(I)—2 La(I′)	—	2.986	2.846 (11)	2.856 (10)
La(I′)—3 O(3)	—	2.642 (18)	2.537 (16)	2.565 (15)
La(I′)—3 O(II′)	—	2.46 (7)	2.49 (6)	2.51 (5)
Na(I′)—3 O(3)	2.421 (18)	2.325 (20)	—	—
Na(I′)—3 O(II′)	2.66 (7)	—	—	—
Na(II)—3 O(2)	2.406 (10)	2.445 (9)	2.445 (13)	2.413 (16)
Na(II)—3 O(4)	—	—	—	2.788 (13)

of T—O(3) with T—O(1), T—O(2) and T—O(4) in our samples, T—O(3) is indeed longer, except for d-41LNaY. In dehydrated 68LaNaY, the T—O(3) distance is the longest one owing to site I′ being mainly occupied by lanthanum ions.

Xenon Adsorption Isotherm

The adsorption isotherms of xenon adsorbed on a series of dehydrated LaNaY zeolites at 22 °C are shown in Fig. 1. The amount of xenon adsorbed at equilibrium pressure decreases with increasing La content on LaNaY. At low xenon loadings, the adsorption isotherms are assumed to follow Henry's law, $\Theta = kP_{Xe} = \rho_{Xe}/\rho_{Xe\infty}$, $k\rho_{Xe\infty} = K = \rho_{Xe}/P_{Xe}$, where ρ_{Xe} and $\rho_{Xe\infty}$ are the xenon loadings at an equilibrium xenon pressure, P_{Xe}, and at a very high xenon pressure, respectively. The slopes of the isotherms, K, and the corresponding Henry's equilibrium constant, k, decrease linearly with decreasing Na content as shown in Fig. 2. Similar behaviour is shown for HNaY with varying Na^+/H^+ ratios (Fig. 1); here the effect of H^+ should be much smaller than that of Na^+ on xenon adsorption. These results suggest that Na^+ ions may be the adsorption centres for xenon atoms in LaNaY and HNaY. The adsorption-isotherm constant depends on the number of Na^+ ions located in supercages after dehydration. The occupancy of site II by Na^+ decreases with increasing La content, as also confirmed by X-ray diffraction. Xenon adsorption is a sensitive and useful tool for studying cation locations and occupancies at sites in Y zeolite supercages.

^{129}Xe NMR

Variations of the ^{129}Xe NMR chemical shift with concentration of adsorbed xenon in the supercage, are shown in Fig. 3. The intercept and slope for NaY zeolite are very similar to those obtained by Fraissard and Ito.[17] The intercepts of the above plots for Xe on LaNaY increase with increasing La content, and at low xenon concentrations the plot becomes parabolic for the higher La-containing sample. The difference between the intercepts for the 69LaNaY and NaY samples is 8 ppm. At higher xenon concentrations, the chemical shift *vs.*

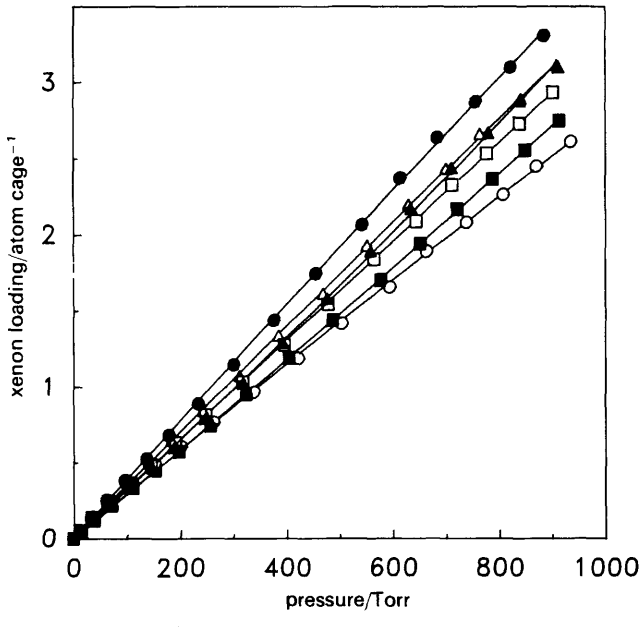

Fig. 1 Isotherms for xenon on NaY (●), LaNaY with 21(△), 41(□) and 69(○) La exchange (%), and on NH_4NaY with 41(▲) and 75(■) NH_4 exchange (%)

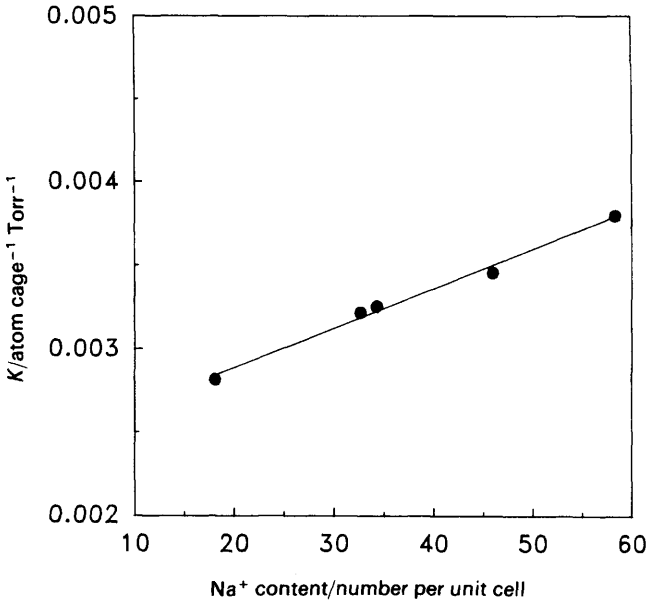

Fig. 2 Variation of the slopes (K) of xenon adsorption isotherms at low xenon loadings with Na^+ content in LaNaY zeolites

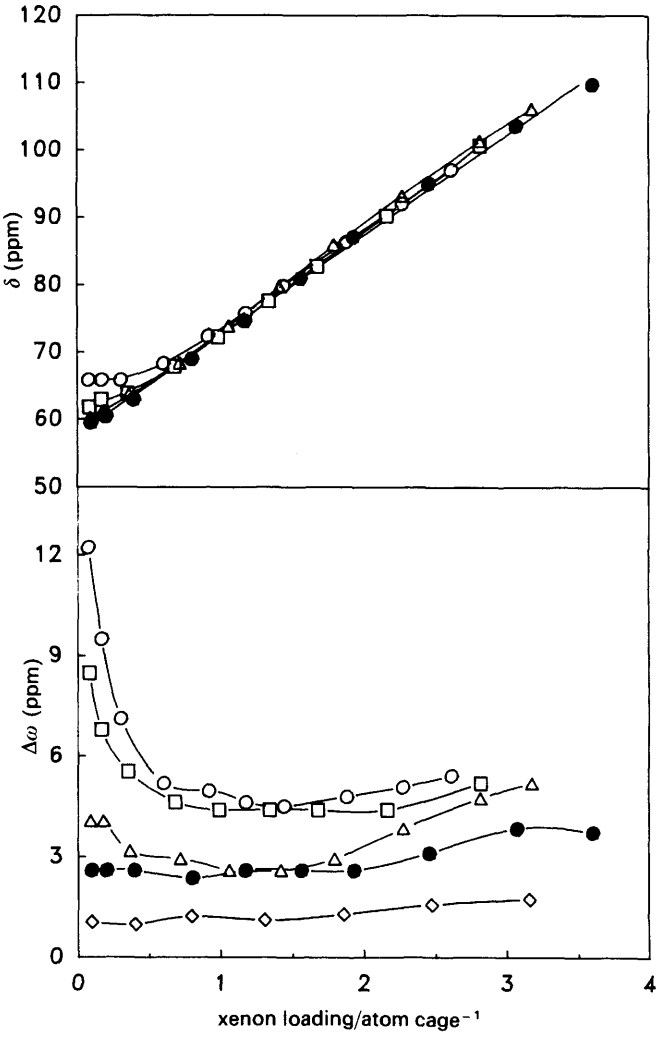

Fig. 3 Chemical shifts, δ, and linewidths at half height, $\Delta\omega$, of ^{129}Xe NMR signals *vs.* number of xenon atoms adsorbed per supercage for NaY (●), 66CsNaY (◇) and LaNaY with 21 (△), 41 (□) and 69 (○) La exchange (%)

xenon density plots of LaNaY coincide almost completely with the straight line obtained for the NaY zeolite.

The ^{129}Xe chemical shift of xenon adsorbed on a zeolite can be described as the sum of four terms[18]

$$\delta(Xe) = \delta_0 + \delta_s + \delta_e + \delta_{Xe}\rho_{Xe} \quad (1)$$

where δ_0 is the chemical shift of the reference and is taken as zero in this report, δ_s depends on the interaction between xenon and the cage wall and corresponds to the chemical shift at zero xenon loading and δ_e is the term from the electric field due to the cations and the aluminosilicate framework; according to Ito and Fraissard,[17] this term is independent of the number of Na^+ ions in the supercages of Y zeolites. The last term arises from Xe–Xe collision and is important in determining the slope of the δ *vs.* ρ_{Xe} plot which can be used to characterize the intraframework void space of the supercage.

The second term of eqn. (1), being characteristic of a xenon–cage wall interaction, depends only on the electronic environment of the supercage wall. The slight increase of δ_s with increasing La content (Fig. 3) may be accounted for by the existence of a few strong adsorption sites created by La^{3+} ions inside the small sodalite and hexagonal prism cavities. The variation of the ^{129}Xe NMR linewidths at half-height [$\Delta\omega = \Delta H(k/Hz)/\omega_0$, ω_0 is the resonance frequency] with xenon loading and La content is illustrated in Fig. 3. For low xenon concentrations, ^{129}Xe linewidths were found to increase with decreasing xenon coverage on LaNaY, but were found to be independent of xenon concentration on NaY and CsNaY. This may be the result of inhomogeneous field broadening owing to the existence of a few strong adsorption sites on the supercage wall of LaNaY which do not occur on the monovalent cation forms of zeolite. The xenon nucleus experiences a large fluctuation of the local magnetic field during the adsorption–desorption process. At low xenon loadings, the linewidth is mainly derived from Xe–wall and Xe–cation collisions, while Xe–Xe collisions are the dominant factors at high xenon loadings. The linewidths at the same xenon loadings are in the order LaNaY > NaY > CsNaY, which implies that the uniformity of the electronic environment of the supercages is in the order LaNaY > NaY > CsNaY. The electric and magnetic fields of the supercages turned out to be more homogeneous in the presence of Cs^+, which is isoelectronic with xenon.[30]

According to X-ray data, all or most of the La^{3+} ions migrate irreversibly into the sodalite or hexagonal prism cages after dehydration and they have very little influence on the intrasupercage void space. This also reflected by the slope of the δ *vs.* ρ_{Xe} plot (Fig. 3) which, at high xenon loading, is identical to that of NaY.

This work was supported in part by the National Science Council of R.O.C. The authors thank Prof. W. J. Mortier (K.U. Leuven, Belgium) for the computer software on XRD data analysis.

References

1 P. B. Venuto and E. T. Habib Jr., *Fluid Catalytic Cracking with Zeolite Catalysts*, Marcel Dekker, New York, 1979.
2 I. Halasz, J. Horvath, T. Mandy, L. Schmidt and E. Tasnadi, in *Proc. Intl. Symposium on Zeolites, Portoroze, 1984*, ed. B. Držaj, S. Hočevar and S. Pejovnik, Elsevier, Amsterdam, 1985, p. 393.
3 A. Corma, V. Fornés, F. V. Melo and J. Herrero, *Zeolites*, 1987, **7**, 559; W. Kladnig, *J. Phys. Chem.*, 1976, **80**, 262.
4 P. A. Jacobs and J. B. Uytterhoeven, *J. Chem. Soc., Faraday Trans. 1*, 1973, **69**, 373; J. W. Ward, *J. Catal.*, 1969, **13**, 321.
5 A. K. Cheetham, M. M. Eddy and J. M. Thomas, *J. Chem. Soc., Chem. Commun.*, 1984, 1337.
6 M. L. Costenoble, W. J. Mortier and J. B. Uytterhoeven, *J. Chem. Soc., Faraday Trans. 1*, 1977, **73**, 466.
7 J. V. Smith, J. M. Bennett and E. M. Flanigen, *Nature (London)*, 1967, **215**, 241.
8 J. Scherzer, J. L. Bass and F. D. Hunter, *J. Phys. Chem.*, 1975, **79**, 1194.
9 L. V. C. Rees and Z. Tao, *Zeolites*, 1986, **6**, 234.
10 J. M. Bennett and J. V. Smith, *Mater. Res. Bull.*, 1968, **3**, 865; 1969, **4**, 343.
11 K. J. Chao and J. Y. Chern, *J. Phys. Chem.*, 1989, **93**, 1401.
12 E. F. T. Lee and L. V. C. Rees, *Zeolites*, 1987, **7**, 143.
13 L. B. Welsh and S. L. Lambert, in *Characterization and Catalyst Development*, ed. S. A. Bradley, M. J. Gattuso and R. J. Bertolacini, American Chemical Society, Washington D.C., 1989, *Am. Chem. Soc. Symp.*, **411**, 262.
14 H. S. Sherry, *J. Colloid Interface Sci.*, 1969, **28**, 288.
15 H. S. Sherry, *Colloid Interface Sci.*, 1976, **5**, 321.
16 L. Moscou and M. Lakemam, *J. Catal.*, 1970, **16**, 173.
17 T. Ito and J. Fraissard, *J. Chem. Phys.*, 1982, **76**, 5225.
18 J. Fraissard and T. Ito, *Zeolites*, 1988, **8**, 350; *J. Chem. Phys.*, 1986, **83**, 441; *J. Chem. Soc., Faraday Trans. 1*, 1987, **83**, 451.
19 T. T. P. Cheung, C. M. Fu and S. Wharry, *J. Phys. Chem.*, 1988, **92**, 5170.
20 K. J. Chao, S. H. Chen and M. H. Yang, *Fres. Z. Anal. Chem.*, 1988, **311**, 418.
21 L. R. Gellens, W. J. Mortier, R. A. Schoonheydt and J. B. Uytterhoeven, *J. Phys. Chem.*, 1981, **85**, 2783.
22 W. J. Mortier, *Proceedings Symposium Accuracy in Powder Diffraction*, N.B.S. Spec. Publ. 567, Washington D.C., 1980, p. 315.
23 C. J. Jameson, *J. Chem. Phys.*, 1975, **63**, 5296.
24 W. J. Mortier, E. van den Bossche and J. B. Uytterhoeven, *Zeolites*, 1984, **4**, 41.
25 E. Dendooven, W. J. Mortier and J. B. Uytterhoeven, *J. Phys. Chem.*, 1984, **88**, 1916.
26 J. J. V. Dun and W. J. Mortier, *J. Phys. Chem.*, 1988, **92**, 6740.
27 E. Dempsey *J. Phys. Chem.*, 1969, **73**, 3660.
28 R. M. Barrier, *Zeolites and Clay Minerals as Solvents and Molecular Sieves*, Academic Press, London, 1978, p. 87.
29 R. M. Barrier and P. J. Cram, *Molecular Sieve Zeolites—II*, American Chemical Society, 102, 1971, p. 105.
30 S. H. Chen, Ph.D. Thesis, University of Tsinghua, ROC, 1990.

Paper 1/01187A; *Received* 13*th March*, 1991